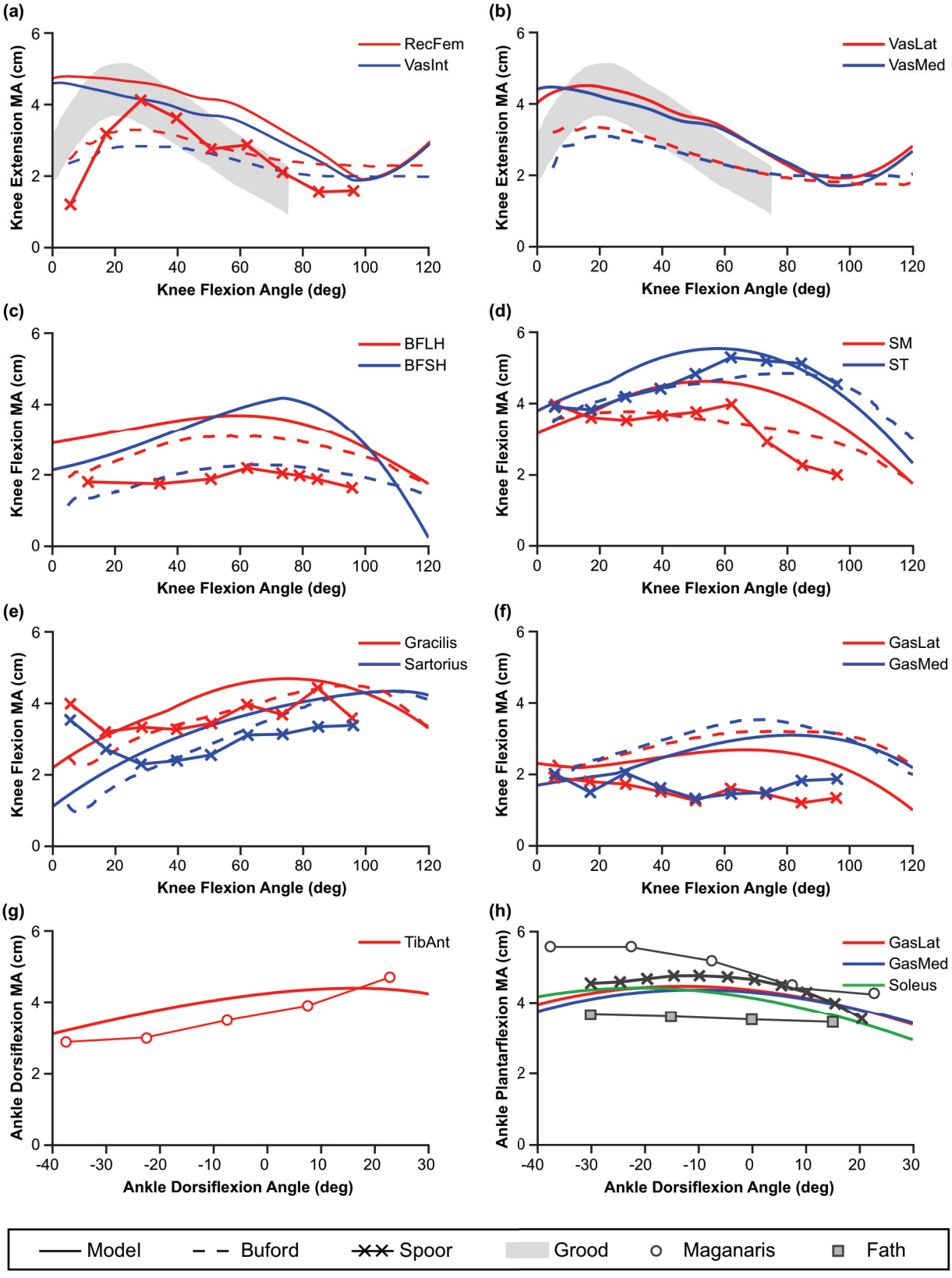

Supplemental Fig. 1. Model moment arms of the major knee and ankle flexors and extensors compared to experimental data. Model moment arms vs. knee flexion angle are shown for (a) rectus femoris (RecFem), vastus intermedius (VasInt), (b) vastus lateralis (VasLat), vastus medialis (VasMed), (c) biceps femoris long head (BFLH) and short head (BFSH), (d) semimembranosus (SM), semitendinosus (ST), (e) gracilis, sartorius, (f) gastrocnemius lateralis (GasLat) and medials (GasMed). Moment arms vs. ankle dorsiflexion angle are shown for (g) tibialis anterior (TibAnt) and the (h) triceps surae (GasLat, GasMed, and Soleus). The model moment arms (solid lines) were compared to experimentally measured moment arms by Grood *et al.* (shaded) [33], Buford *et al.* (dashed lines) [32], Spoor *et al.* (×) [34], Maganaris *et al.* (o) [36], and Fath *et al.* (□) [35].

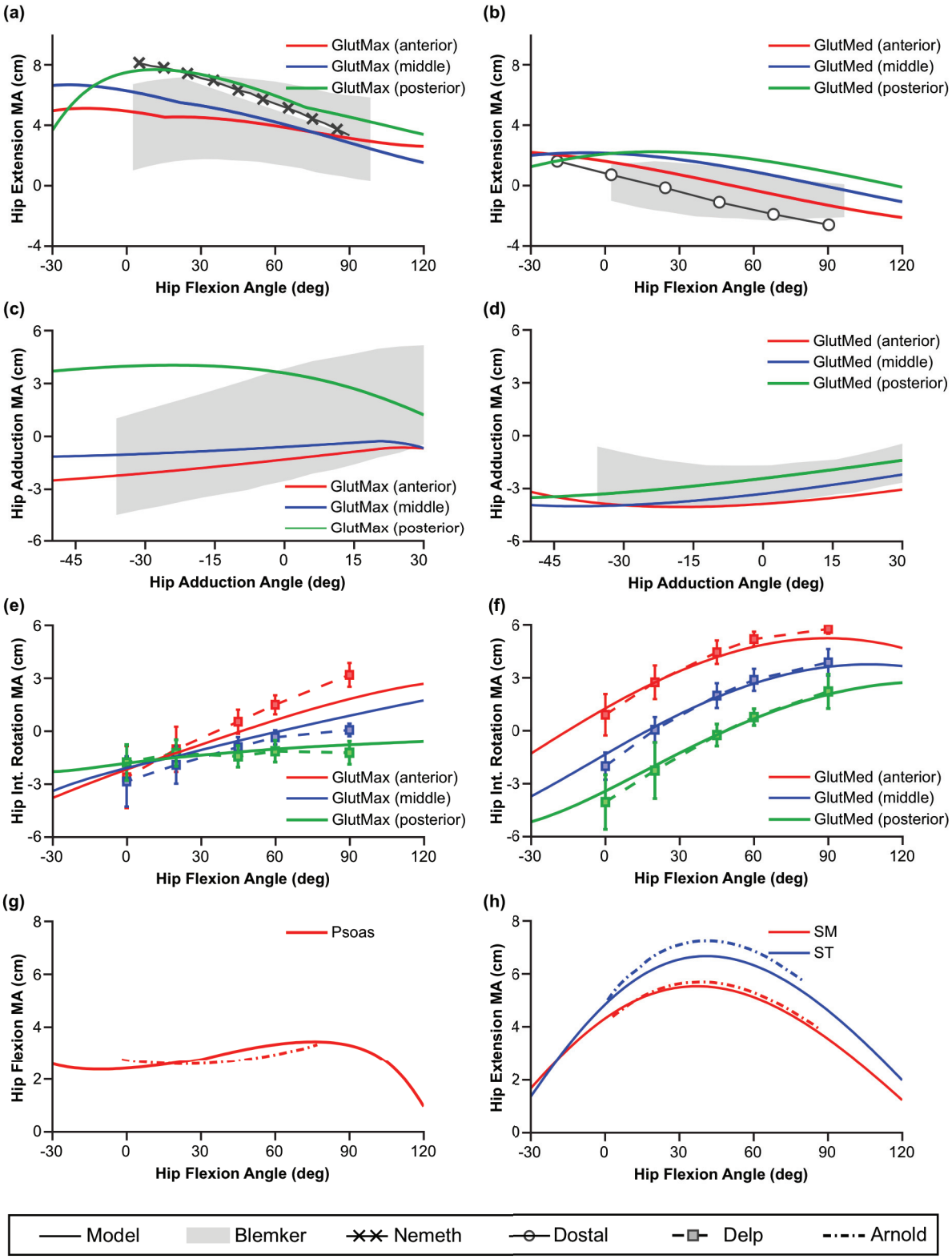

Supplemental Fig. 2. Model moment arms of major hip flexor/extensors, abductors/adductors, and internal/external rotators compared to experimental data. Model hip extension moment arms vs.hip flexion angle are shown for (a) gluteus maximus (GlutMax) and (b) gluteus medius (GlutMed). Model hip adduction moment arms vs. hip adduction angle are shown for (c) gluteus maximus and (d) gluteus medius. Model hip internal rotation moment arms vs. hip flexion angle are shown for (e) gluteus maximus and (f) gluteus medius. Model hip flexion/extension moment arms vs. hip flexion angle are shown for (g) psoas and the (h) semimembranosus (SM) and semitendinosus (ST). The model moment arms (solid lines) were compared to finite element simulated moment arms by Blemker *et al.* (shaded) [12] and experimentally measured moment arms by Nemeth *et al.* (x) [37], Dostal *et al.* (o) [38], Delp *et al.* (□) [39], and Arnold *et al.* (dash-dot) [40].

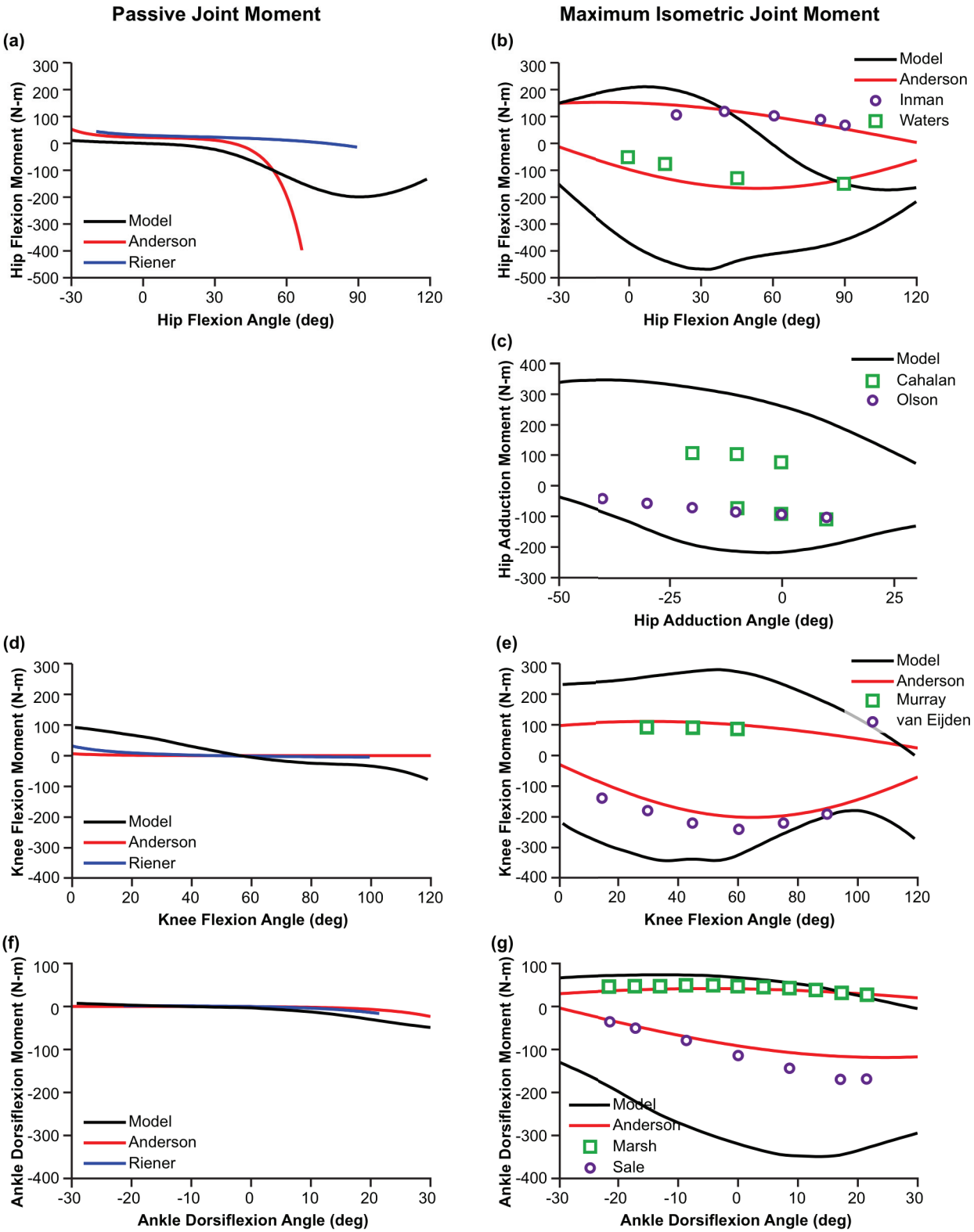

Supplemental Fig. 3. Model passive joint moments and maximum isometric joint moments compared to experimental data. Hip flexion moments, (a) and (b), were computed with the knee fixed at 10° flexion. Knee flexion moments, (d) and (e), were computed with the hip fixed at 70° flexion. Ankle flexion moments, (f) and (g), were computed with the knee fixed at 80° flexion. In each case, unspecified joint angles were fixed at 0°. Passive joint moments for hip flexion (a), knee flexion (d), and ankle dorsiflexion (f) were calculated by summing the passive moments produced by all muscles crossing the respective joint. Active joint moments were computed for hip flexion/extension (b), hip adduction/abduction (c), knee flexion/extension (e), and ankle dorsiflexion/plantarflexion (g) by summing the maximum isometric moment produced by all agonist muscles and the passive moment produced by the antagonist muscles. Results are plotted against experimental data reported by Anderson *et al*. [59], Riener *et al*. [74], Inman *et al*. [60], Waters *et al*. [61], Cahalan *et al*. [62], Olson *et al*. [63], Murray *et al*. [64], Van Eijden *et al*. [65], Marsh *et al*. [66], and Sale *et al*. [67].

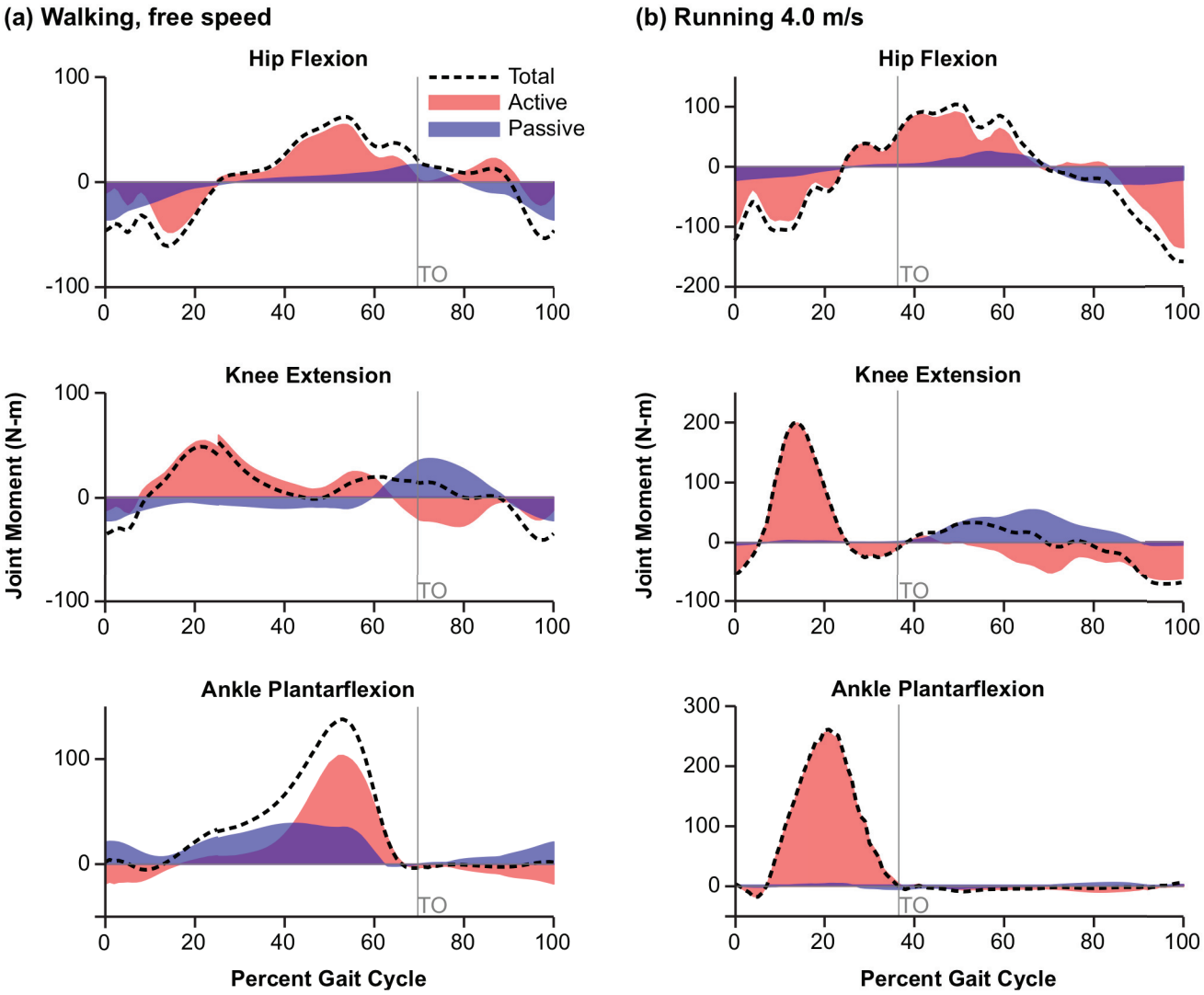

Supplemental Fig. 4. Passive and active muscle-generated joint moments for one gait cycle of walking and running. Total muscle-generated joint moments (dashed line) for the hip, knee, and ankle joint during muscle-driven simulations of (a) walking and (b) running were broken down into the passive (blue) and active (red) joint moments. Toe-off (TO) is indicated with the gray vertical line.

SUPPLEMENTAL TABLE I
MUSCULOTENDON PARAMETERS WITH EXPECTED VARIATION

Muscle	Abbreviation	Optimal force (N) (± S.D.)	Optimal fiber length (cm) (± S.D.)	Tendon slack length (cm) [a] (± S.D.)	Pennation angle (°) (± S.D.)
Adductor brevis	addbrev	626 (130)	10.3 (1.4)	3.5* (1.7)	6.6 (3.4)
Adductor longus	addlong	917 (220)	10.8 (2.0)	13.2 (2.6)	7.9 (3.9)
Adductor magnus[be]					
Adductor magnus (distal)	addmagDist	597 (131)	17.7 (3.4)	8.7* (3.5)	11.2 (5.5)
Adductor magnus (ischial)	addmagIsch	597 (131)	15.6 (3.0)	21.6 (3.2)	9.6 (4.7)
Adductor magnus (middle)	addmagMid	597 (131)	13.8 (2.6)	4.7* (2.6)	11.9 (5.8)
Adductor magnus (proximal)	addmagProx	597 (131)	10.6 (2.0)	4.0* (2.2)	17.8 (8.7)
Biceps femoris long head	bflh	1313 (402)	9.8 (2.6)	32.5 (2.8)	10.1 (4.9)
Biceps femoris short head	bfsh	557 (158)	11.0 (2.1)	10.6* (2.6)	15.1 (4.5)
Extensor digitorum longus[ce]	edl	603 (115)	6.9 (1.1)	36.9 (1.5)	12.5 (3.4)
Extensor hallucis longus[ce]	ehl	286 (51)	7.5 (1.1)	32.7 (1.4)	11.3 (2.7)
Flexor digitorum longus	fdl	423 (148)	4.5 (1.1)	37.9 (1.1)	12.9 (4.6)
Flexor hallucis longus	fhl	908 (273)	5.3 (1.3)	35.4 (1.3)	14.8 (4.3)
Gastrocnemius lateral head	gaslat	1575 (404)	5.9 (1.0)	37.6 (1.1)	12.0 (3.3)
Gastrocnemius medial head	gasmed	3116 (727)	5.1 (1.0)	39.9 (1.1)	9.5 (4.3)
Gluteus maximus[be]					
Gluteus maximus (superior)	glmax1	984 (181)	14.7 (2.4)	4.9* (4.0)	20.3 (24.3)
Gluteus maximus (middle)	glmax2	1406 (260)	15.7 (2.6)	6.8* (4.4)	21.0 (25.3)
Gluteus maximus (inferior)	glmax3	948 (175)	16.7 (2.7)	7.0* (4.9)	21.9 (26.3)
Gluteus medius[be]					
Gluteus medius (anterior)	glmed1	1093 (279)	7.3 (1.6)	5.6* (1.7)	18.1 (15.2)
Gluteus medius (middle)	glmed2	765 (195)	7.3 (1.6)	6.5* (1.7)	18.1 (15.2)
Gluteus medius (posterior)	glmed3	871 (222)	7.3 (1.6)	4.5* (1.7)	18.1 (15.2)
Gluteus minimus[bef]					
Gluteus minimus (anterior)	glmin1	374 (48)	6.8 (n/a)	1.6* (n/a)	10.0 (n/a)
Gluteus minimus (middle)	glmin2	395 (59)	5.6 (n/a)	2.6* (n/a)	0.0 (n/a)
Gluteus minimus (posterior)	glmin3	447 (86)	3.8 (n/a)	5.1 (n/a)	1.0 (n/a)
Gracilis	grac	281 (70)	22.8 (4.4)	17.2* (5.5)	9.9 (3.1)
Iliacus	iliacus	1021 (219)	10.7 (1.9)	9.6* (2.0)	16.0 (6.1)
Peroneus brevis[de]	perbrev	521 (109)	4.5 (0.7)	14.8 (0.8)	11.8 (3.2)
Peroneus longus[de]	perlong	1115 (220)	5.1 (0.6)	33.2 (0.8)	14.2 (5.3)
Piriformis[f]	piri	1030 (287)	2.6 (n/a)	11.5 (n/a)	10.0 (n/a)
Psoas	psoas	1427 (306)	11.7 (1.7)	10.0* (2.2)	12.3 (3.9)
Rectus femoris	recfem	2192 (473)	7.6 (1.3)	44.8 (1.4)	12.4 (3.5)
Sartorius	sart	249 (43)	40.3 (4.6)	12.4* (5.9)	1.5 (2.1)
Semimembranosus	semimem	2201 (645)	6.9 (1.8)	34.8 (2.1)	14.6 (3.6)
Semitendinosus	semiten	591 (148)	19.3 (4.1)	24.7 (5.2)	13.8 (5.4)
Soleus	soleus	6195 (1606)	4.4 (1.0)	27.7 (1.0)	21.9 (8.0)
Tensor fascia latae[f]	tfl	411 (125)	9.5 (n/a)	44.9 (n/a)	3.0 (n/a)
Tibialis anterior	tibant	1227 (205)	6.8 (0.8)	24.0 (1.0)	11.2 (3.7)
Tibialis posterior	tibpost	1730 (358)	3.8 (0.5)	28.1 (0.7)	13.0 (4.2)
Vastus intermedius	vasint	1697 (437)	9.9 (2.0)	20.2 (2.3)	3.6 (3.7)
Vastus lateralis	vaslat	5149 (1025)	9.9 (1.8)	22.1 (1.9)	14.5 (5.7)
Vastus medialis	vasmed	2748 (701)	9.7 (2.3)	20.0 (2.8)	24.2 (7.6)

Musculotendon parameters. Muscle physiological cross sectional areas (PCSAs) were calculated from muscle volumes measured by Handsfield *et al.* [26] in healthy, young subjects. Optimal fiber lengths were measured by Ward *et al.* [20] in cadaver subjects. Pennation angle at optimal fiber length was calculated using pennation angle measurements in cadavers by Ward *et al.* and adjusted for fiber length using the constant-volume assumption made by Millard *et al*. Tendon slack length was set in the model to match normalized fiber length measurements reported by Ward *et al.*

[a]Tendons were modeled as rigid when the tendon slack length was less than the muscle optimal fiber length. Rigid tendons are indicated with a (*).

[b]Muscle volume was only available for the whole muscle. Total muscle volume for each muscle was divided equally between the muscle-tendon units using the same volume distribution as in the model by Arnold *et al.* [15].

[c]Muscle volume was only available for extensor digitorum longus, extensor hallucis longus, and peroneus tertius combined. Peroneus tertius was not included in our model. The total muscle volume was divided between extensor digitorum longus and extensor hallucis longus using the volume proportions used by Arnold *et al.* [15].

[d]Muscle volume was only available for peroneus brevis and peroneus longus combined. The total muscle volume was divided between the two using the volume proportions used by Arnold *et al.* [15].

[e]Mean and standard deviation of experimental muscle volume fraction, optimal fiber length, and/or pennation angle were not reported separately for each muscle-tendon compartment (see notes b,c,d). To do the variability analysis described below, standard deviations of relevant experimental measures were assigned to each muscle-tendon compartment to maintain the coefficient of variation reported for the whole muscle [20], [26].

[f]Experimental variation in fiber length and pennation angle were not reported by Ward *et al.* [20]. Variation in optimal fiber length, tendon slack length, and pennation angle at optimal fiber length was not computed. Variation in optimal force was computed only with respect to variation in muscle volume.

Notes associated with Supplemental Table I. Expected variation in muscle optimal force (F_o^m), optimal fiber length (l_o^m), tendon slack length (l_s^t), and pennation angle at optimal fiber length (α_o) was computed based on the reported variation in optimal fiber length, pennation angle (α) and normalized fiber length ($\tilde{l}^m$) at a specified pose [20], and muscle volume fraction (ϕ^m) [26].

Optimal fiber force:

$$F_o^m = \sigma_o^m \frac{\phi^m V_{total}}{l_o^m}$$

Variance was computed based on a first-order Taylor expansion as shown below

$$\left(\sigma_{F_o^m}\right)^2 \approx \left(\frac{\partial F_o^m}{\partial \phi^m}\Big|_{nom} \sigma_{\phi^m}\right)^2 + \left(\frac{\partial F_o^m}{\partial l_o^m}\Big|_{nom} \sigma_{l_o^m}\right)^2$$

where

- $\sigma_{F_o^m}$ is the standard deviation in optimal fiber force,
- σ_{ϕ^m} is the standard deviation in muscle volume fraction reported by Handsfield *et al*. [26], and
- $\sigma_{l_o^m}$ is the standard deviation in optimal fiber length reported by Ward *et al*. [20].

Optimal fiber length:
Standard deviation of this parameter was taken directly from Ward *et al*. [20].

Tendon slack length:

$$l_s^t = f(l_o^m, \tilde{l}^m, \alpha_o)$$

Standard deviation of this parameter was computed using a Monte-Carlo simulations with 10,000 trials per muscle-tendon unit with $l_o^m \sim N(\mu_{l_o^m}, \sigma^2_{l_o^m})$, $\tilde{l}^m \sim N(\mu_{\tilde{l}^m}, \sigma^2_{\tilde{l}^m})$, and $\alpha_o \sim N(\mu_{\alpha_o}, \sigma^2_{\alpha_o})$, where

- $\mu_{l_o^m}, \mu_{\tilde{l}^m}, \mu_{\alpha_o}$ are the mean values for these parameters used in the model,
- $\sigma_{l_o^m}$ is the standard deviation in optimal fiber length reported by Ward *et al*. [20],
- $\sigma_{\tilde{l}^m}$ is the standard deviation in the passive normalized fiber length at 7° hip flexion, 2° hip abduction, 0° knee flexion, and 20° plantarflexion (see text, Methods *B*) reported by Ward *et al*. [20], and
- σ_{α_o} is the standard deviation in pennation angle at optimal fiber length, computed below.

Pennation angle at optimal fiber length:

$$\alpha_o = \sin^{-1}\left(\tilde{l}^m \sin\alpha\right)$$

Variance was computed based on a first-order Taylor expansion as shown below

$$\left(\sigma_{\alpha_o}\right)^2 \approx \left(\frac{\partial \alpha_o}{\partial \tilde{l}^m}\Big|_{nom} \sigma_{\tilde{l}^m}\right)^2 + \left(\frac{\partial \alpha_o}{\partial \alpha}\Big|_{nom} \sigma_{\alpha}\right)^2$$

where

- σ_{α_o} is the standard deviation in pennation angle at optimal fiber length,
- σ_{α} is the standard deviation in pennation angle at the normalized fiber length reported by Ward *et al*. [20], and
- $\sigma_{\tilde{l}^m}$ is as defined earlier [20].